Desalination and Water Treatment
www.deswater.com

doi: 10.5004/dwt.2018.23061

132 (2018) 20–29
November

Humidification-dehumidification spray column direct contact condenser—Part II: Experimental co-current flow

Aly Karameldin, Loula A. Shouman, Dalia A. Fadel*

Reactors Department, Nuclear Research Center, Atomic Energy Authority, P.O. 13759 Inshas, Cairo, Egypt, email: AlyKarameldin@hotmail.com (A. Karameldin), loulashouman@yahoo.com (L.A. Shouman), dalia_shaaban@windowslive.com (D.A. Fadel)

Received 1 February 2018; Accepted 1 September 2018

ABSTRACT

An experimental set up is designed and constructed to investigate the Humidification-Dehumidification (HDH) Co-current Direct Contact Condenser spray column (CDCC). The results obtain that, the inlet hot humid air temperature has a great influence on the condensate. As the inlet humid air temperature rise from 40 to 70°C the condensate increases approximately more than 4 times at constant cooled spray water and hot humid air mass fluxes. The increase of humid air mass fluxes from 0.158 to 0.316 kg/m^2·s redoubles the condensate at the same inlet humid air temperature. The increase of the cooled spray water mass fluxes increases the condensate, where there is no radical increase of condensate at liquid mass flux above 5 kg/m^2·s. Therefore, there is an optimum value of the spray water mass flux. Also, the results show good agreement between experimental measurements and theoretical predictions of condensate, where the deviation doesn't exceed 7%. Comparison between co-current and counter current flow of the condensate is theoretically obtained, which reveals no advantage between the two systems. A case study of a contiguous co-generation electricity and water desalination by HDH in Nuclear or conventional Power Plants show that the HDH productivity can reach 15 m^3/d·m^2.

Keywords: Humidification-dehumidification; Co-current flow-spray column; Direct contact condenser; Contiguous co-generation

1. Introduction

Desalination technologies are currently used throughout the world and have been under development for the past century. Humidification dehumidification desalination (HDH) has drawn an interest over the past two decades. HDH is a relatively is a low grade energy desalination technology in which water vapor diffuses into low humid air from saline water (humidification). The water vapor is condensed from the saturated humid air to produce fresh water (dehumidification). The HDH is characterized by operating at low temperature and can be driven by low grade waste heat, enabling the production of unlimited freshwater supply.

The previous studies focused on the performance evaluation, modeling, parametric studies and empirical correlations developed for the HDH unit. Saadawy et al. [1] studied the concept of a novel seawater desalination system that is configured by a humidification–dehumidification unit based on the vapor-compression process (HDD-TVC) and summarized the previous investigations on HDD design and performance. A review study has been done on different type of HDH systems by Kabeel et al. [2] to throw light on thermal modeling for various type of HDH distillation system. These two review summarizes some of the different variants of the HDH from number of researches [3–14]. This summary shows that the main concern of operating conditions of all these investigations was; temperature range from 15 to 92°C, water stream range from 0.0001 to 4.5 kg/s, and humid air stream range from 0.00013 to 0.32 kg/s. Narayan, et al. [15] provided a comprehensive review of the solar-driven humidification–dehumidification (HDH) desalination. Previous studies investigated many different variations on the HDH cycle. The performance parameters which enable comparison of the various versions of the HDH cycle had been defined

*Corresponding author.

and evaluated. The principal components of the HDH system were also reviewed and compared.

Recently, the direct contact has concerned in several studies. Jin et al. [16] compared between direct contact evaporation in both co-current and counter-current humid gas flow and studied the effect of various parameters to evaluate the heat transfer performance. Baqir et al. [17] obtained the performance of the spray column direct contact heat exchanger under the influence of various operational conditions. Direct contact dehumidification column had been investigated experimentally and theoretically to decrease dehumidifier size and cost by Tow and Lienhard [18]. The studies of direct-contact condenser without packed bed were performed on surface and bubble column. A direct contact dehumidification in bubble column was tested experimentally by Tow and Lienhard [19] and the results are presented in terms of heat flux and effectiveness. An HDH system consisting of a packed-bed humidifier and a multi-tray bubble column dehumidifier was modeled and investigated by Chehayeb et al. [20]. The effect of the mass flow rate ratio on the performance of a fixed-size system was studied and its effect on the entropy generation and the driving forces for heat and mass transfer. In addition, generalized energy effectiveness for heat and mass exchangers was defined. Niroomand et al. [21] introduced a direct contact dehumidification process used in humidification–dehumidification system instead of using the conventional indirect condensers. In the purposed system, air was dehumidified by spraying cold water into the hot and humid air stream. The freshwater production, efficiency and effects of various parameters on the performance of the system were investigated. Results showed that direct contact dehumidifier had a good potential in desalination of seawater which can resolve many operational problems of indirect condensers. Klausner et al. [22,23] described and discussed the direct contact condenser of a diffusion driven desalination facility.

A counter current falling droplets spray type direct contact condenser was theoretically investigated by the present authors [24]. A mathematical model is developed to predict the thermal performance of the falling droplet counter-current flow direct contact condenser. It should be pointed out that the range of the operating parameters was quite small in the column length, humid air temperature and the mass flux. The input temperatures of humid air are varied from 34.2 to 80°C and the inlet spray water droplets temperature are varied from 25 to 45°C. Meanwhile, the humid air and spray water mass fluxes are varied from 0.25 to 3.5 kg/m^2·s and from 1.25 to 50 kg/m^2·s respectively. In this study, the results showed that the column length has a great effect on the performance of the spray condenser. At a column height of 2, 5, 10, and 20 m the humidity of the outlet humid air decreases by 72, 89, 97, and 99%, respectively. The humid air temperature has a great influence on the condensate; meanwhile the temperature difference between the humid air and sprayed water has less effect. Also, a case study of a contiguous co-generation electricity and water in nuclear power plants (NPP) showed that at the optimal operating conditions, the productivity by HDH can reach more than 15 m^3/d·m^2 [24].

The objective of the present work is to parametrically study the co-current direct contact condenser spray column (CDCC) (without packing) theoretically and experimentally. The effect of the various parameters on the condensate such as; the inlet humid air temperature, the mass flux of spray cooling water and the humid air mass flux will be investigated. Validity of the theoretical model will be experimentally performed through experimental setup measurements.

2. Theoretical model

The evaluation of the CDCC (without packing) is performed through the parametric study of the effects of the operating parameters. One-dimensional, quasi-steady mathematical model for a falling droplet is urbanized for the CDCC. The conservation of mass, momentum, and energy of a moving droplet are adopted to the differential control volume for co-current flow as shown in Fig. 1. The conservation equations for mass, momentum, and energy of a moving droplet [22,23] are mentioned briefly as following:

2.1. Variation of droplet size-mass transfer

The cold fresh-spray water droplets at temperature T_d will increase in size due to the condensation of the vapor, which is contained in the gas stream at a higher temperature T_a. Considering a single droplet in the control volume, the rate of change in the droplet radius, R_d, as it flows down the condenser chamber can be calculated as:

$$\frac{dR_d}{dZ} = \frac{\gamma_d\left(\rho_v\left(T_a\right) - \rho_{sat}\left(T_d\right)\right)}{\rho_w v_d} \tag{1}$$

where z is the vertical coordinate, measuring from where droplets are introduced; ρ_w is the spray water droplet density (kg/m^3); ρ_v is the vapor density at temperature T_a; ρ_{sat} is the vapor density corresponding to temperature T_{sat};

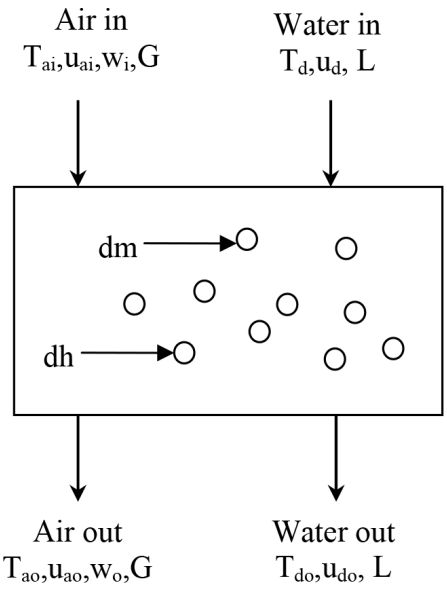

Fig. 1. Unit control volume mass and energy balances.

R_d and υ_d are the radius and velocity of the droplet; and γ_d is the mass transfer coefficient (m/s).

The mass transfer coefficient γ_d is empirically calculated from:

$$\gamma_d = \frac{D\left(2+0.5\mathrm{Re}^{1/2}\right)}{2R_d} \tag{2}$$

where D is the diffusion coefficient of water vapor.

2.2. Droplet velocity - momentum transfer

To predict the droplet velocity υ_d, Newton's second law is applied. The rate of change of momentum of the continuously accelerating droplet considers the aerodynamic drag force and the gravitational force:

$$\frac{d\nu_d}{dz} = \frac{g}{\nu_d} - C_{drag}\frac{\rho_a\left(\nu_d - u_{air}\right)^2}{2m_d\nu_d}\pi R_d^2 - \frac{3}{R_d}\nu_d\frac{dR_d}{dz} \tag{3}$$

where C_{drag} is the aerodynamic drag coefficient on the droplet based on a standard empirical correlation, u_a is the velocity of air/vapor mixture; m_d is the droplet mass; and g is the gravitational acceleration.

2.3. Droplet temperature - energy transfer

The droplet temperature is affected by the convective heat by convective heat transfer of air/vapor flow around the droplet and the phase change. The rate of change of droplet volume-average (bulk) temperature due to condensation of water vapor on the droplet surface is given by:

$$\frac{dT_d}{dz} = \frac{3\left\{U\left(T_a - T_d\right) + \gamma_d\left(\rho_v\left(T_a\right) - \rho_{sat}\left(T_d\right)\right)\left(h_{fg} - C_{pw}T_d\right)\right\}}{\rho_w C_{pW}\nu_d R_d} \tag{4}$$

where U is the heat transfer coefficient; h_{fg} is the latent heat of vaporization at T_a; and C_{pw} is the specific heat of the spray water droplet.

The heat transfer coefficient, U is estimated from:

$$Nu = 2R_d U/k_a \tag{5}$$

2.4. Air temperature variation- energy transfer

Similarly, conservation of energy and mass on the air-vapor mixture yields expression for the change in the humid air temperature.

$$\frac{dT_a}{dz} = -\frac{4\pi R_d^2 N_d\left\{U\left(T_a - T_d\right) - h_l\gamma_d\left(\rho_v\left(T_a\right) - \rho_{sat}\left(T_d\right)\right)\right\}}{\rho_{mix}CP_{mix}U_a} \tag{6}$$

where h_l is the specific liquid enthalpy at T_a; N_d is the specific number of droplets (number of droplets per unit volume) at any axial location.

2.5. Mass flux of condensed vapor

The rate of condensed liquid into the spray water droplets is given by:

$$\dot{m}_{cond.vap} = \left(\omega_0 - \omega_f\right)G/\left(1+\omega_0\right) \tag{7}$$

the absolute specific humidity ω, as:

$$\omega = \frac{0.622\varphi P_{sat}\left(T_a\right)}{p - \varphi Psat\left(T_a\right)} \tag{8}$$

For an air/vapor mixture, $P_{sat}(T_a)$ is the saturation pressure at T_a and the relative humidity φ.

The deduced equations calculate the variation of droplet size, droplet velocity, droplet temperature and air/vapor mixture temperature distributions, and humidity ratio (w) along the height of the CDCC. The model assumptions, the whole equations and the solution methodology are explained in details in [24].

3. Experimental set up

A schematic diagram of the humidification dehumidification experimental facility setup is shown in Fig. 2, the experimental setup contains two main columns. The first is the bubbling humidification column (bubbling column) (12) and the second is the CDCC dehumidification column (17). The humidification and dehumidification columns are attached by a PVC elbow (14) and the loop is described in details.

3.1. Humidification section

Dry air is supplied from an air compressor (1) through a filter. The air pressure and flow rate is controlled by a pressure regulator (2) attached to a mass flow meter. The inlet air state is determined by pressure, temperature and relative humidity (3). The pressure of inlet air is measured using pressure controller (Omega model PRG–501) of accuracy 0.05% and sensitivity 0.005 psig. The relative humidity and the temperature of inlet air are measured by using a hygrometer (Cole-Parmer model 3700–500) of accuracy ±2% and response time of 10 s. The air mass flow rate is measured by a flow meter (Omega model FMA–600) of accuracy ±1% full scale.

The bubbling section consists of 1m stainless steel pipe. The top and the bottom of the pipe are attached with two stainless steel flanges of 1 cm thickness. Two stainless steel heater of 1.5 kW (8, 9) are inserted in the button flange, elevating the inlet dry air temperature to a certain value. The heated air passes through a none-return valve, and distributed through a set of spiral nozzles (16) attached to two air strainers (10). The air is forced to pass through the bubbling column, wherever mass and heat transfers from the heated liquid to the flowing air resulting in the air humidification process.

The humidification column (12) comprises; 1m stainless steel pipe long and 5 m polyvinyl chloride pipes with 25 cm ID. As shown in the figure, the flange comprises two

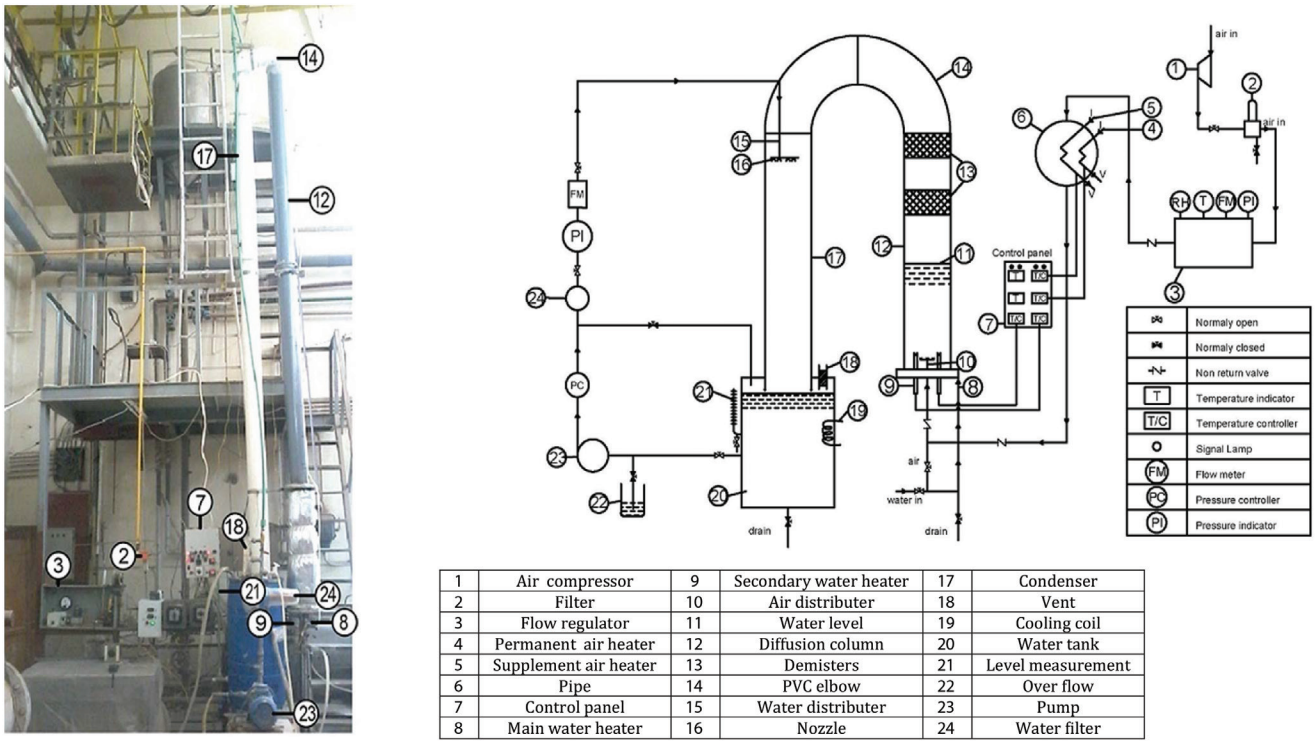

1	Air compressor	9	Secondary water heater	17	Condenser
2	Filter	10	Air distributer	18	Vent
3	Flow regulator	11	Water level	19	Cooling coil
4	Permanent air heater	12	Diffusion column	20	Water tank
5	Supplement air heater	13	Demisters	21	Level measurement
6	Pipe	14	PVC elbow	22	Over flow
7	Control panel	15	Water distributer	23	Pump
8	Main water heater	16	Nozzle	24	Water filter

Fig. 2. Schematic diagram and photograph for the experimental setup.

temperature controllers' attached to the electric heaters, two demisters (13) to remove the mist carryover, and water supply and blow down tubes. The two heaters are used to raise the water temperature to certain value, one coarse and another fine. The heaters electric power supplies are controlled by two temperature controllers allocated in the control panel (7). The feedback temperature to each controller is supplied with a type K thermocouple. The control panel is designed and constructed to control the water temperatures in the humidifier (12) as well as the humid air entering the condenser (dehumidifier) (17). A temperature probe of 27 K–type thermocouples, is centered axially through the whole length of the column(dehumidifier) (17), to measure the temperature distribution along the column.

3.2. Dehumidification section

The CDCC dehumidifier (17) consists of PVC pipe 6m long with ID 25 cm. At the top of condenser, a set of nozzles (16) are attached to a water spray distributor (15). The sprayed water is pumped (23) from the product tank (20) through a filter, and pressure and flow controllers. The temperature of sprayed water tank (20). The tank is equipped with level measurement (21) and air vent through a demister (18). The pumped spraying water is filtered (24) and equipped with a pressure indicator and a flow meter (model–7650 series manufactured by king instrument) with accuracy ±2% and repeatability 0.5%.

The humid saturated air flows at the top of the CDCC's dehumidifier at an elevated temperature and humidity. In which the water vapor tends to condense onto the sprayed water droplets due heat and mass exchanged through the column height. As the humid air flows down through the column it is cooled down and the dehumidification process takes place. At the outlet of CDCC, the temperature and humidity of the discharge air are measured with a duct mounted (FF-IND-10V type) hygrometer with an accuracy of ±2% and response time 10 s.

In the present study, the input temperature of humid air (T_{ai}) varies from 40 to 70°C and the input cold spray water temperature varies from 21 to 29°C (according to the ambient temperature). The air mass fluxes (G) change from 0.15 to 0.35 kg/m^2.s and water mass fluxes (L) change 1.7 to 7 kg/m^2.s and the both are limited due to the experimental setup availability.

It is worth to mention that the CDCC column height is chosen to be 6m which meets the available lab facility. Meanwhile, the recommended column height from a previous study has been indicated the column height of 5–10 m gives the maximum attainable condensate at the different operating conditions [24].

4. Results and the discussion

The performance of the co-current direct contact condenser spray column (CDCC) is evaluated experimentally and theoretically by studying the effects of the spray column operating parameters.

Fig. 3 shows the variation of condensate flow rate with inlet humid air temperature and different humid air mass flow rates. Also, it shows the comparison between the condensate flow rate of experimental measurements and

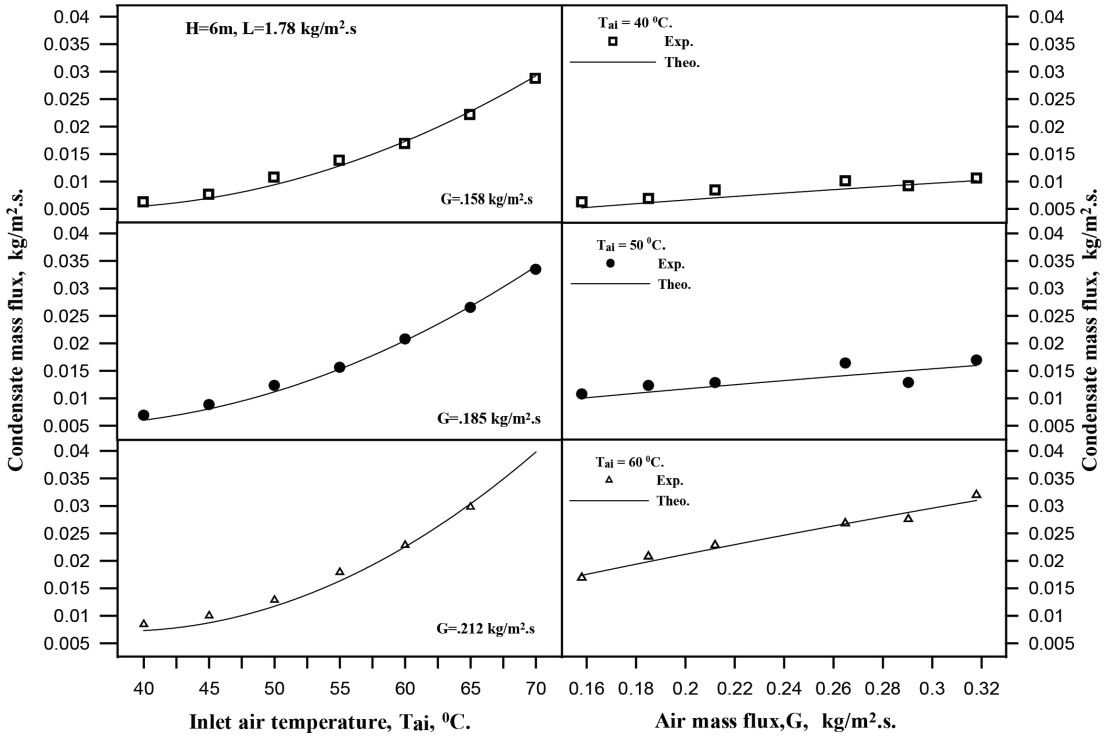

Fig. 3. The variation of the condensate mass flux with the humid air inlet temperature, at different air mass flux.

theoretical model predictions. As shown in the figure, the increase of humid air mass flux and/or inlet humid air temperature increase the condensate flow rate. When the inlet humid air temperature increases from 40 to 70°C, the condensate increases more than 4 times (for the same humid air and spray water fluxes). The higher inlet humid air temperature, the higher temperature difference (between humid air and spray water) the higher condensate. The figure also illustrates that the increase of humid air mass fluxes from 0.158 to 0.316 kg/m²·s, increases the condensate approximately 2 times (at the same inlet humid temperature). From these results, the inlet humid air temperature has the prime of importance on the condensate process than the humid air and water mass fluxes. The figure also shows that, the deviation between experimental and theoretical results do not exceed ±5%.

Fig. 4 shows the variation of outlet humid air temperature with inlet humid air temperature and humid air mass fluxes. As seen from the curves, for a fixed sprayed water mass flux and, the outlet humid air temperature is strongly dependent on inlet humid air temperature. The outlet humid air temperature increases with the increase of the inlet humid air temperature (at a constant sprayed water and the humid air mass flux). Moreover, the effect of the humid air mass flux on the outlet humid air temperature is studied also at different inlet humid air temperature. From the figure, the increase of the humid air mass flux (at the inlet humid air temperature 40°C) slightly increases the outlet humid air temperature. Which indicates that the vapor content of the inlet humid air almost condensed? For the inlet humid air temperature of 50 and 60°C, doubling the humid air mass flux will increase the outlet humid air temperature by only 20%. In which, the increase of humid air outlet temperature is the measure of its vapor content. A good agreement between the experimental and theoretical model results is observed, where the maximum deviation do not exceed ±8%.

The effect of the inlet humid air temperature and spray water mass fluxes on the condensate flow rate are depicted in Fig. 5. The measured condensate is confirmed with the theoretical model. The results show that, as the humid air temperature increases and/or the spray water mass flux increases, the condensate mass flux increases. These significant increases are referred to the rise of temperature difference between humid air (40–70) and spray water (20–29). Therefore, additional increase of inlet humid air temperature, results in increase of the condensate mass flux. Meanwhile, the increase of the spray water mass fluxes above 5 kg/m²·s no radical increase of condensate mass flux is it is observed. Therefore, there is an optimum value of the spray water mass flux that can't condenses more vapor for certain air mass flux and inlet humid air temperature.

The variation of outlet humid air temperature with water mass flux at different inlet humid air temperature is presented in Fig. 6. The increase of inlet humid air temperature from 40 to 70°C increases the outlet humid air temperature from around 25 to 30°C (at constant sprayed water and humid air mass fluxes). Noting that, the increase of inlet humid air temperature increases the humidity content of its. Also, the increase of the spray water mass flux decreases the outlet humid air temperature. The figure shows that as the spray water mass flux increases 3 times, the outlet humid air temperature increases about 16%, which

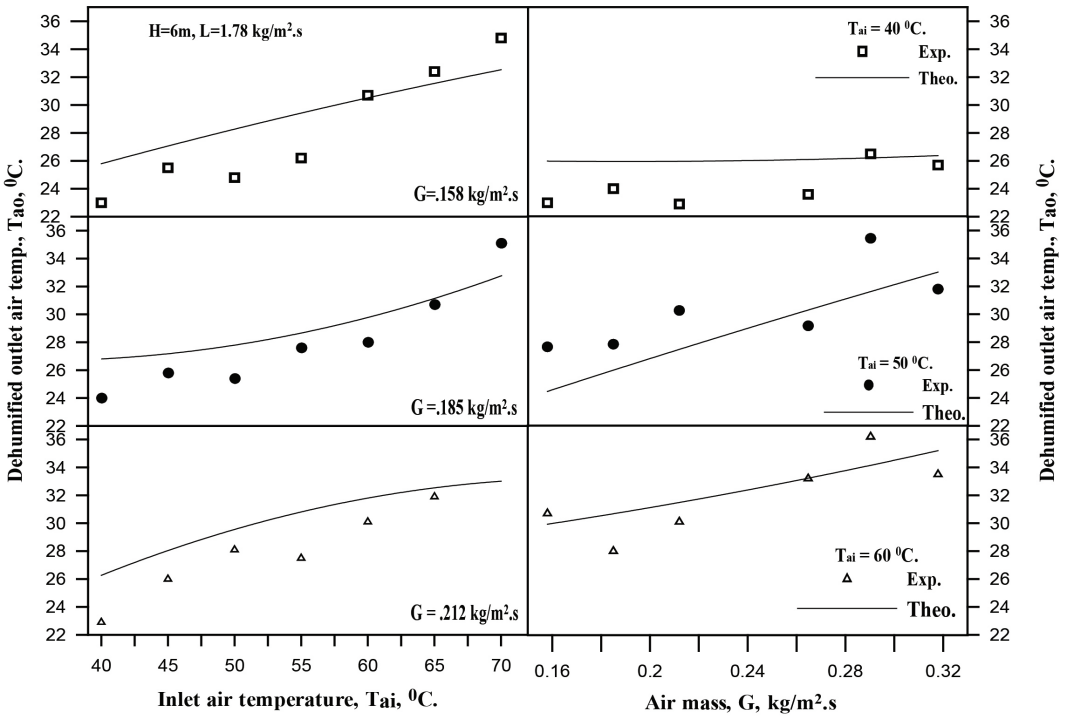

Fig. 4. The variation of the humid outlet and inlet air temperature, at different air mass flux.

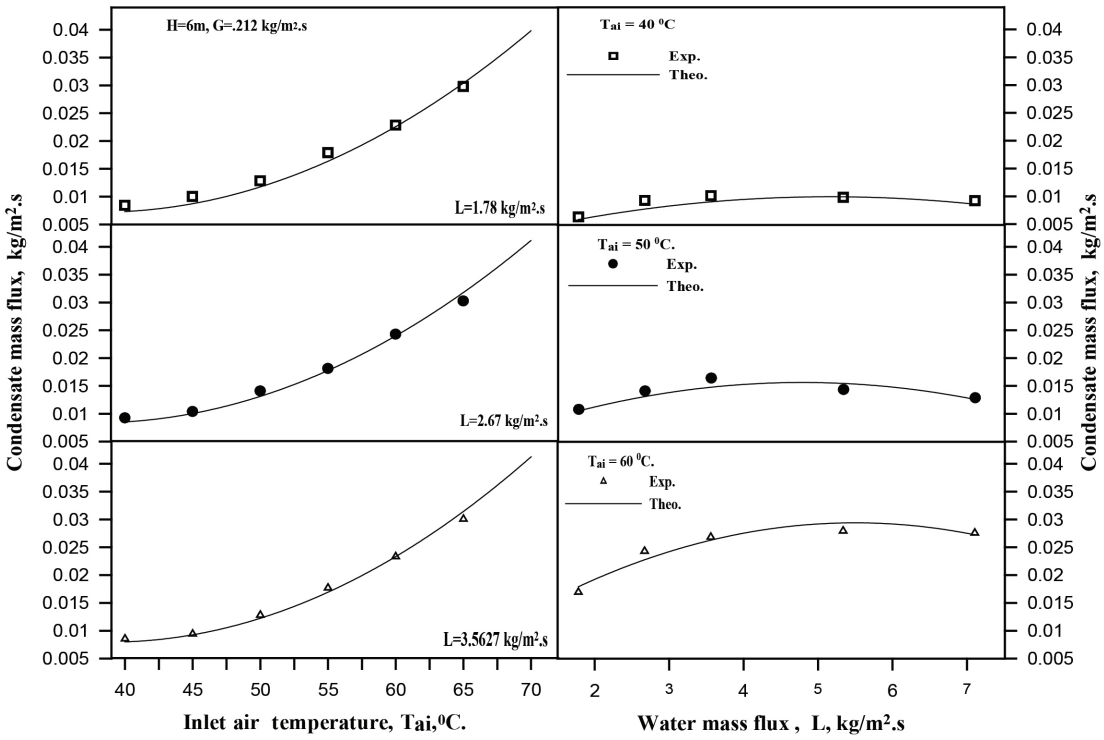

Fig. 5. The variation of the condensate mass flux with the humid air inlet temperature, at different water mass flux.

indicates that the spray water mass flux has less effect. The figure also shows that, a good agreement between the experimental measurements maximum deviation do not exceed ±7%.

4.1. De-humidifier performance

The performance of the CDCC can be evaluated by the effectiveness of the de-humidifier which is defined

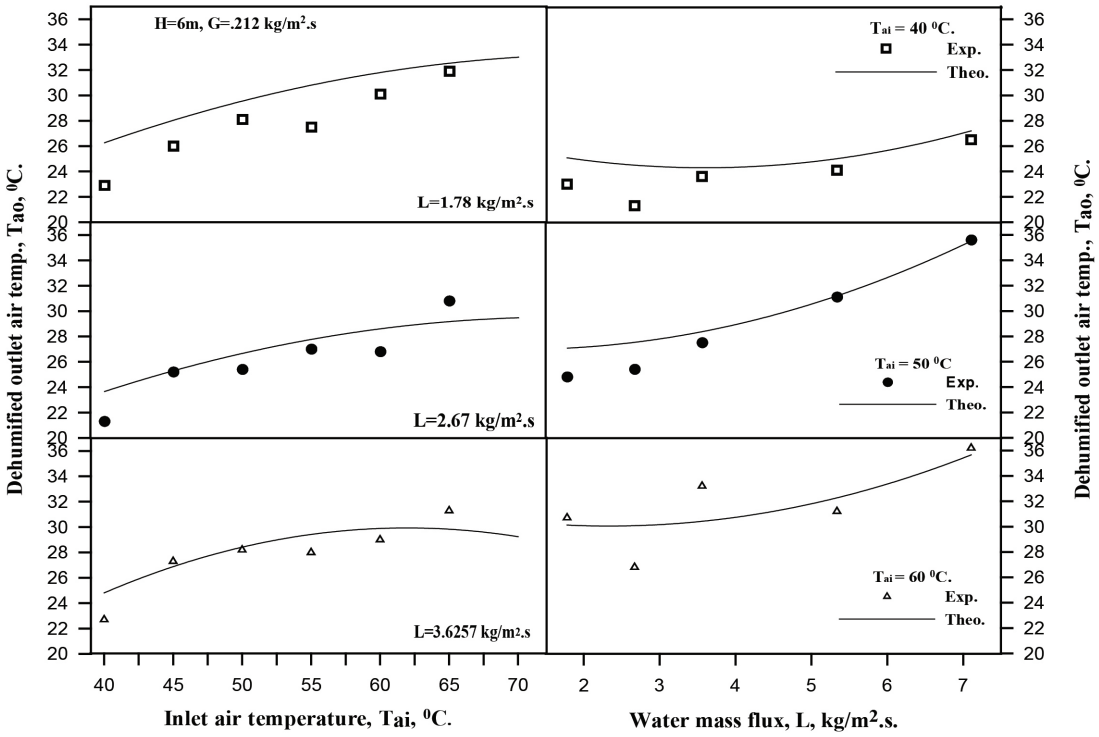

Fig. 6. The variation of the humid outlet and inlet air temperature, at different water mass flux.

as the ratio of actual enthalpy change of either stream (Δh) to maximum possible enthalpy change (Δh_{max}). The effectiveness of CDCC is calculated theoretically from:

$$\varepsilon = \frac{\Delta h}{\Delta h_{\max}} = \frac{h_{a,in} - h_{a,out}}{h_{a,in} - h_{w,in}}$$

where $h_{a,in}$ and $h_{a,out}$ are the enthalpy of inlet air and outlet air of the dehumidifier. $h_{w,in}$ is the enthalpy of saturated moist air at the temperature $T_{w,in}$.

Fig. 7 shows the variation of effectiveness with humid air and water mass fluxes at different inlet humid air temperature. As shown in the figure, for constant spray water mass flux, the effectiveness decreases by 8% approximately with the increase of the humid air mass fluxes from 0.158 to 0.316 kg/m²·s. This decrease due to that, the increase of humid air mass fluxes increases the vapor content and so the outlet humid air temperature increases. Therefore, (at constant sprayed water flux and humid air inlet temperature), doubling the humid air mass flux decrease the actual heat transfer rate and the effectiveness. Also, as mentioned before, the increase of the spray water mass flux, for constant humid air mass flux, increases the condensate and so decreases the outlet humid air temperature. Therefore, with the increase of the spray water mass fluxes from 1.78 to 7.1 kg/m²·s the effectiveness increases by 12% approximately. At the constant sprayed water and humid air mass fluxes the effect of inlet humid air temperature on effectiveness illustrate that, no radical increase of effectiveness is observed.

4.2. Comparison between co-current and counter current flow in CDCC

The validation of the theoretical model is performed experimentally in the co-current flow in CDCC, which shows a good agreement between the experimental and theoretical values. Therefore, the mathematical model is valid to study different cases for comparison between the co-current and counter current direct contact condenser [24]. Fig. 8 gives these comparisons of the condensate mass fluxes, at different inlet humid air temperature and temperature difference between humid air and sprayed water.

As shown in Fig. 8a, at T_d = 25°C (droplets of the sprayed water), the variations of the condensate mass flux at the inlet humid air temperature of 70°C is greater than 6 times that of 40°C, for both co-current and counter current. While in Fig. 8b, when the temperature difference is kept constant at 10°C, the condensate increases by about 4 times corresponding to a humid air temperature rises from 40 to 70°C. The figure also shows that, the condensate of the counter current is greater than the co current about 7.5% and 9.3% at inlet humid air temperature 40 and 70°C, respectively, which discloses that no advantage of the two spray types.

4.3. Case Study

As HDH process makes use of low grade energy or waste heat, therefore; the unlimited and massive quantities of rejected heat at the condenser section of a conventional power plant can be directed to drive HDH units. In which the condenser inlet cooling water temperature can varied between 25 to 40°C (day and night, and/or winter and

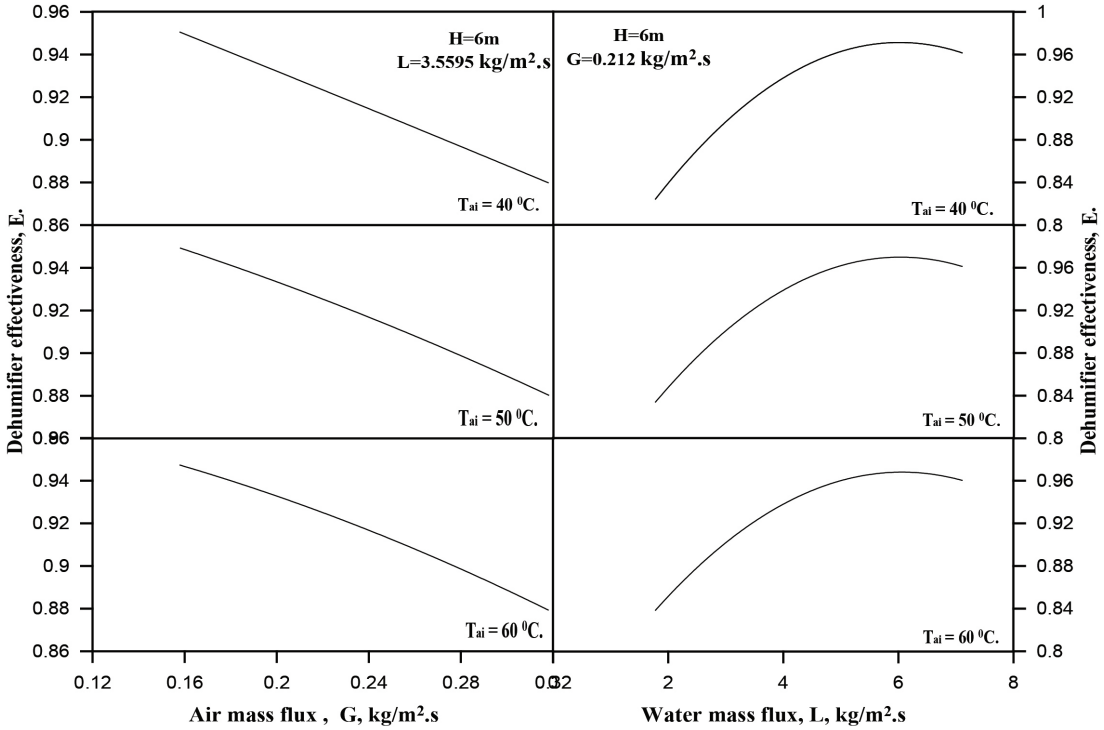

Fig. 7. The variation of the de-humidifier effectiveness with the water and air mass fluxes, at different inlet air temperature.

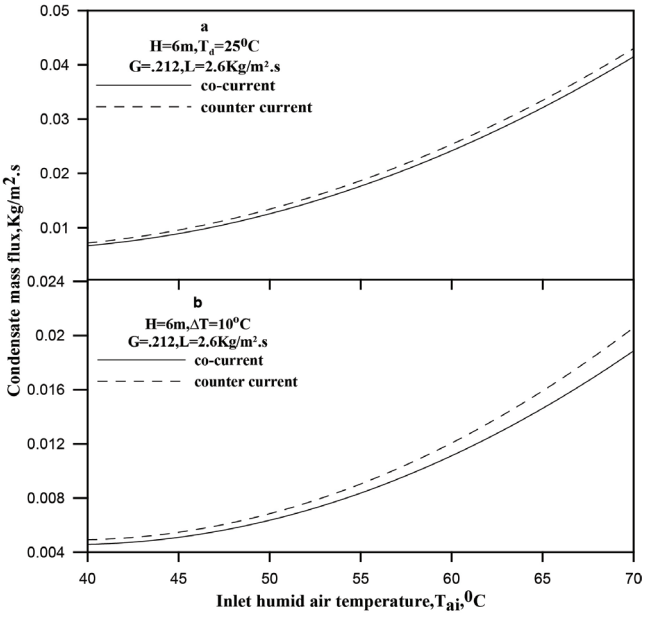

Fig. 8. The comparison of the condensate mass flux for co-current and counter current at different humid air inlet temperature.

summer). Where, the temperature difference between the humid air and the cooling spray water can be by about 10–15°C through the condenser (the heat rejection section). A case study previously performed for the counter current direct contact condenser [24], figured out an approximate formula of the productivity in terms of the humid air temperature and mass flux, and the spray water mass flux.

In the current work, the same case study is theoretically recalculated for the co-current case. Moreover a comparison between the two cases is illustrated in Fig. 9. It is evidently shown from the figure that, the productivity at the maximum profit is increased at the counter current case by 9, 10.5, and 13% than the co-current case at the humid air inlet temperature of 30, 40 and 50°C, respectively. These curves symbolize the design curves of the HDH process linked to a contiguous co-generation for electricity and water production power plants.

It is worth to mention that, an extra heat from the feed water heaters of the conventional power plant or in the secondary circuit nuclear power plants can be used for elevate the inlet temperature of the humid air to 60 and 70°C in this case, the optimal productivity of CDCC can be increased to 19.6441 and 35.7522 $m^3/m^2 \cdot d$, respectively. Moreover, the productivity at the maximum profit is increased about 3 and 5.5 times with escalating the humid air temperature to 60 and 70, respectively; in this case, the economic return of the productivity increase income and the cost of the consumed energy to raise the inlet humid air temperature is improved.

5. Conclusions

Experimental work through an experimental set up is designed and constructed, and theoretical analysis have been presented to study HDH process, which shows a greet agreement between them. In this study it is concluded the humid inlet air temperature to CDCC, is of the prime importance. Meanwhile, the working air mass flux, and

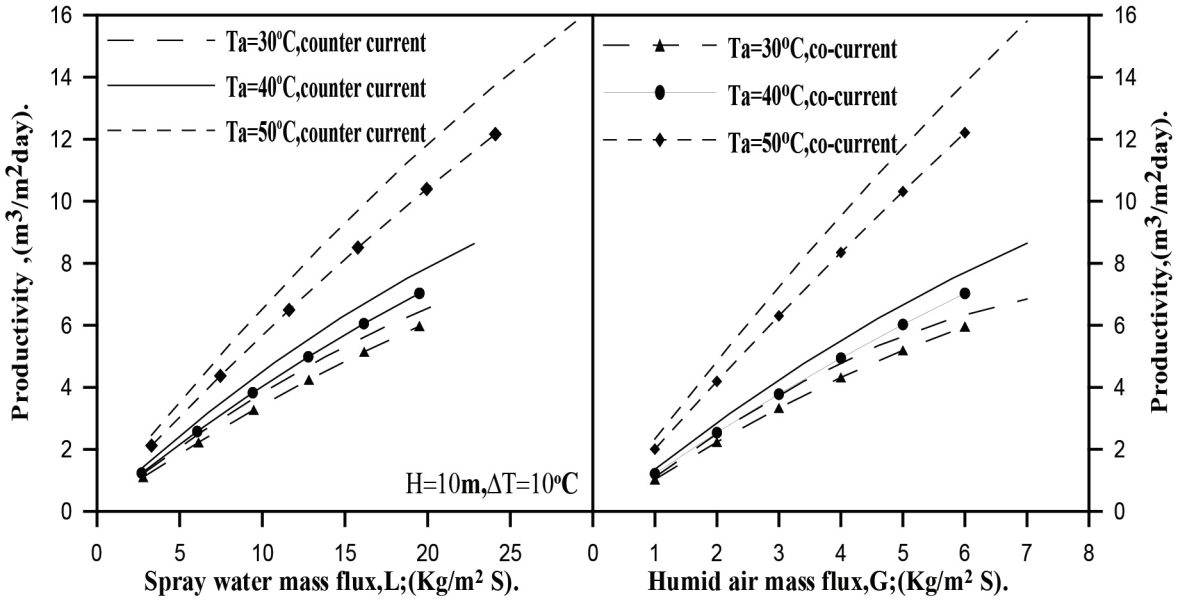

Fig. 9. The comparison of the optimal productivity for co-current and counter current humid air and spray water, at different humid air inlet temperature.

sprayed cooling water temperature and its mass flux, had less importance. When the inlet humid air temperature increases from 40 to 70°C, the condensate increases more than 4 and 6 times (for the same humid air and spray water fluxes), corresponding to constant temperature difference between spayed water and humid inlet air, and constant spayed water temperature, respectively.

The increase of the cooled spray water mass fluxes increases the condensate, where there is no radical increase of condensate at liquid mass flux above 5 kg/m²·s. Therefore, there is an optimum value of the spray water mass flux that can't condense more vapor for certain air mass flux and inlet humid air temperature. The spray water mass flux has less effect, as it increased 3 times, the outlet humid air temperature increases about 16%. The effectiveness for the CDCC is calculated and the effect of cooled spray water and hot humid air mass fluxes on effectiveness is investigated. The effectiveness decreases by 8% approximately with the increase of the humid air mass fluxes and increases by 12% with the increase of the spray water mass fluxes. The design curves of the HDH process have been obtained in a case study by linking a contiguous co-generation for electricity and water production in conventional power plants and shows that the HDH productivity can reach 15 m³/d·m². Moreover, the HDH productivity at the maximum profit is increased by about 3 and 5.5 times with escalating the humid air temperature to 60 and 70°C, respectively; in this case, the economic return of the productivity increase income and the cost of the consumed energy to raise the inlet humid air temperature is improved.

Symbols

A — Cross section area, m²
C_{drag} — Drag coefficient
Cp — Specific heat at constant pressure, kJ/kg·K
D — Diffusion coefficient of water vapor, m²/s
G — Air mass flux, kg/m² s
g — Acceleration due to gravity, m²/s
H — Spray column height, m
h — Enthalpy, kJ/kg
h_{fg} — Latent heat of vaporization, kJ/kg
k — Thermal conductivity, W/m K
L — Spray water mass flux, kg/m²s
m — Mass flow rate, kg/s
m_{drop} — Mass of an individual droplet, kg
N_d — Specific droplet number
p — Pressure, Pa
R_d — Radius of droplet, m
T — Temperature, *K*
υ_d — Droplet velocity, m/s
u — Velocity, m/s
U — Heat transfer coefficient, W/m² K
Z — Column axial Coordinate, m
ω — Absolute humidity
ϕ — Relative humidity
μ — Dynamic viscosity, kg/m s
ρ — Density, kg/m³
γ_d — Mass transfer coefficient for droplet condensation, m/s
ε — Effectiveness

Subscripts

a — Air
d — Droplet
f — Final condition
In,i — Inlet
l — Water in liquid phase
out,a — Outlet
sat. — Saturation
v — Vapor
w — Water

Dimensionless numbers

Re — Reynold number
Nu — Nusslet number

References

[1] M. Saadawy, A. Karameldin, E. Negeed, A novel super-cooled humidification–dehumidification system driven by thermal vapor compression unit for seawater desalination, Int. J. Nucl. Desalin., 3(2) (2008) 186–214.

[2] A.E. Kabeel, H. Mofreh, H. Hamed, Z.M. Omara, S.W. Sharshir, Water desalination using a humidification-dehumidification technique-a detailed review, Nat. Resour. J., 4(3) (2013) 286–305.

[3] A.E. Kabeel, M.S. Emad, El Said, A Hybrid solar desalination system of air humidification-dehumidification and water flashing evaporation part I. A numerical investigation, IWTC16, Istanbul., 7–10 May, (2012).

[4] E.H. Amer, H. Kotb, G.H. Mostafa, A.R. El-Ghalban, Theoretical and experimental investigation of humidification-dehumidification desalination unit, Desalination, 249 (2009) 949–959.

[5] A.S. Nafey, H.E.S. Fath, S.O. El-Helaby, A. Soliman, Solar desalination using humidification-dehumidification processes. Part II. An experimental investigation, Energy Convers. Manage., 45 (2004) 1263–1277.

[6] J.J. Hermosillo, C.A. Arancibia-Bulnes, C.A. Estrada, Water desalination by air humidification: mathematical model and experimental study, Sol. Energy., 86(4) (2011) 1070–1076.

[7] C. Yamali, I. Solmus, A Solar desalination system using humidification-dehumidification process: experimental study and comparison with the theoretical results, Desalination, 220 (2008) 538–551.

[8] Y.J. Dai, H.F. Zhang, Experimental investigation of a solar desalination unit with humidification and dehumidification, Desalination, 130(2) (2000) 169–175.

[9] G. Al-Enezi, H. Ettouney, N. Fawzy, Low temperature humidification-dehumidification desalination process for fossil fuel plants, Energy Conserv. Manage., 47(4) (2006) 470–484.

[10] A. Eslamimanesh, M.S. Hatamipour, Mathematical modeling of a direct contact humidification-dehumidification desalination process, Desalination, 237 (2009) 296–304.

[11] S. Farsad, A. Behzadmehr, Analysis of Solar desalination unit with humidification-dehumidification cycle using DOE method, Desalination, 278 (2011) 70–76.

[12] H.E. Fath, A. Ghazy, Solar desalination using humidification-dehumidification technology, Desalination, 142(2) (2002) 119–133.

[13] J. Orfi, N. Galanis, M. Laplante, Air humidification-dehumidification for water desalination system using solar energy, Desalination, 203 (2007) 471–481.

[14] M. Al-Sahali, M. Hisham, Humidification-dehumidification desalination process: design and performance evaluation, Chem. Engin. J., 143 (2008) 257–264.

[15] G.P. Narayan, M.H. Sharqawy, E.K. Summers, J.H. Linhard, S.M. Zubair, M.A. Antar, The potential of solar-driven humidification dehumidification desalination for small-scale decentralized water production, Renew. Sust. Energy Rev., 14 (2010) 1187–1201.

[16] Y. Jin, R. Hu, Y. Wang, Y. Cui, Y. Liu, Q. Huang, The effect of Dixon rings on direct contact heat transfer performance: Comparison of counter and co-current evaporation, Appl. Therm. Eng., 117 (2017) 762–772.

[17] A. Sh. Baqir, H.B. Mahood, M.S. Hameed, A.N. Campbell, Heat transfer measurement in a three-phase spray column direct contact heat exchanger for utilization in energy recovery from low-grade sources, Energy Conserv. Manage., 126 (2016) 342–351.

[18] E.W. Tow, J.H. Lienhard, Experiments and modeling of bubble column dehumidifier performance, Int. J. Therm. Sci., 60 (2014) 65–75.

[19] E.W. Tow, J.H. Lienhard, Heat flux and effectiveness in bubble column dehumidifiers for HDH desalination, EDT (2016), http:/hdl.handle.net/172.1/87600.

[20] K.M. Chehayeb, G.P. Narayan, S.M. Zubair, J.H. Lienhard, Thermodynamic balancing of a fixed-size two-stage humidification dehumidification desalination system, Desalination, 369 (2015) 125–139.

[21] N. Niroomand, M. Zamen, M. Amidpour, Theoretical investigation of using a direct contact dehumidifier in humidification–dehumidification desalination unit based on an open air cycle, Desal. Water Treat., 54(2) (2015) 305–315.

[22] J.F. Klausner, Y. Li, R. Mei, Innovative fresh water productions process for fossil fuel plants, Annual report, University of Florida, 2004.

[23] J.F. Klausner,Y. Li, R. Mei, Innovative fresh water productions process for fossil fuel plants, Annual report, University of Florida, 2005.

[24] A. Karameldin, L.A. Shouman, D.A. Fadel, Humidification–Dehumidification (HDH) spray column direct contact condenser part I: countercurrent flow, Arab J. Nucl. Sci. Appl., 94(4) (2016) 41–54.